
DRAFT

CMS Paper

The content of this note is intended for CMS internal use and distribution only

2012/06/11

Head Id:

Archive Id: 128758

Archive Date: 2012/06/09

Archive Tag: trunk

Study of the $Z\gamma \rightarrow \nu\nu\gamma$ production at $\sqrt{s} = 7$ TeV

The CMS Collaboration

Abstract

We report the first measurement of the $Z\gamma \rightarrow \nu\nu\gamma$ cross section for the photon transverse momentum $E_T^\gamma > 130$ GeV in pp collisions at $\sqrt{s} = 7$ TeV. The study is done on the data sample corresponding to an integrated luminosity of approximately 5 fb^{-1} . The measured cross section is $57 \pm 11(\text{stat.}) \pm 12(\text{syst.}) \pm 1(\text{lumi.}) \text{ fb}$, which is in a good agreement with the theoretical prediction of $59 \pm 3 \text{ fb}$ at next-to-leading order precision. We also set the most stringent limits on anomalous $ZZ\gamma$ and $Z\gamma\gamma$ triple gauge couplings to date.

This box is only visible in draft mode. Please make sure the values below make sense.

PDFAuthor: J. Damgov, Y. Maravin, S. Shrestha
PDFTitle: Study of the Zgamma production in gamma+MET final state at sqrt(s) = 7 TeV
PDFSubject: CMS
PDFKeywords: CMS, physics

Please also verify that the abstract does not use any user defined symbols

1 The study of the production of a pair of bosons provides an important test of the electroweak
 2 sector of the standard model (SM), as the production is sensitive to trilinear gauge boson self-
 3 interaction couplings or TGCs, a consequence of the non-Abelian nature of the $SU(2) \times U(1)$
 4 symmetry. The values of these couplings are fully fixed in the SM, and thus, any measured
 5 deviation from the SM prediction would be an indication of new physics. New symmetries,
 6 or new particles would give rise to non-zero values of these couplings that would result to an
 7 excess of the cross section over the SM prediction, especially for high energy bosons. Thus,
 8 in most searches for anomalous TGCs the differential cross section of the photon transverse
 9 energy is used as a sensitive observable.

10 In this article, we describe a study of the $Z\gamma$ production that is sensitive to trilinear gauge
 11 couplings (TGCs) $Z\gamma\gamma$ and $ZZ\gamma$. As photons cannot couple to neutral particles at leading
 12 order (LO), these trilinear gauge couplings are zero in the SM. The most general Lorentz- and
 13 gauge-invariant $ZV\gamma$ vertex is described by four coupling parameters, h_i^V , ($i = 1..4$) [1], where
 14 V is either a Z boson or a photon. The first two couplings ($i = 1, 2$) are CP-violating, while the
 15 latter two are CP-conserving. If one uses the differential cross section to interpret the results in
 16 terms of h_i^V then the sensitivity between CP-violating and CP-conserving couplings is similar.
 17 Therefore, the results are usually interpreted in terms of CP-conserving couplings h_3 and h_4 .
 18 Any anomalous TGC results in a violation of the unitarity at sufficiently high energy, which
 19 often fixed by assuming a form-factor energy dependence of these couplings. In this study we
 20 do not make any assumption on the energy dependence, and provide a measurement of the
 21 TGCs averaged for the energy range available at LHC.

22 In this study, we chose the Z boson decay to a pair of neutrinos. The sensitivity to anomalous
 23 TGCs in $Z\gamma \rightarrow \nu\nu\gamma$ process is expected to be much higher compared to Z boson decay modes
 24 to charged leptons. One of the reasons is that no identification requirements are needed for the
 25 final state particles except for significant imbalance of the transverse energy. The branching
 26 fraction of Z boson decay to a pair of neutrinos is also three times larger than a decay to a
 27 particular charged lepton pair, as we cannot distinguish between neutrino generations. Finally,
 28 $\nu\nu\gamma$ final state can be produced only through initial state radiation process, where a photon
 29 is emitted by an initial state parton, or through the anomalous TGC vertex, while $Z \rightarrow \ell^+\ell^-$
 30 processes can have a photon produced by the final state charged lepton. An absence of final
 31 state radiation processes further increases the sensitivity to anomalous TGCs in $\nu\nu\gamma$ final state.
 32

33 The search for anomalous $Z\gamma\gamma$ and $ZZ\gamma$ was performed by Tevatron [2], [3], LEP experi-
 34 ment [4], [5] and by CMS and ATLAS. Based on 36 pb^{-1} of CMS (2010 data), limits on h_3^γ and
 35 h_4^γ are 0.07 and 0.0005 while h_3^Z and h_4^Z are 0.06 and 0.0005 respectively [6]. The obtained sensi-
 36 tivity to h_3^γ and h_4^γ is 0.027 and 0.00021, and that for h_3^Z and h_4^Z is 0.026 and 0.00021, respectively
 37 from ATLAS [7].

38 This search uses data collected with the Compact Muon Solenoid (CMS) detector described
 39 in details elsewhere [8]. The momenta of charged particles are measured using a silicon pixel
 40 and strip tracker that is immersed in a 3.8 T superconducting solenoid, and covers the pseu-
 41 dorapidity range $|\eta| < 2.5$. The pseudorapidity is $\eta = -\ln[\tan(\theta/2)]$, where θ is the polar
 42 angle measured relative to the counterclockwise-beam direction. The tracker is surrounded
 43 by a crystal electromagnetic calorimeter (ECAL) and a brass-scintillator hadron calorimeter
 44 (HCAL). Both measure particle energy depositions and consist of a barrel assembly and two
 45 endcaps that provide coverage in the range of $|\eta| < 3.0$. A steel/quartz-fiber Cherenkov for-
 46 ward detector (HF) extends the calorimetric coverage to $|\eta| < 5$. Muons are measured in gas
 47 detectors embedded in the steel return yoke outside of the solenoid. Data used in this analysis

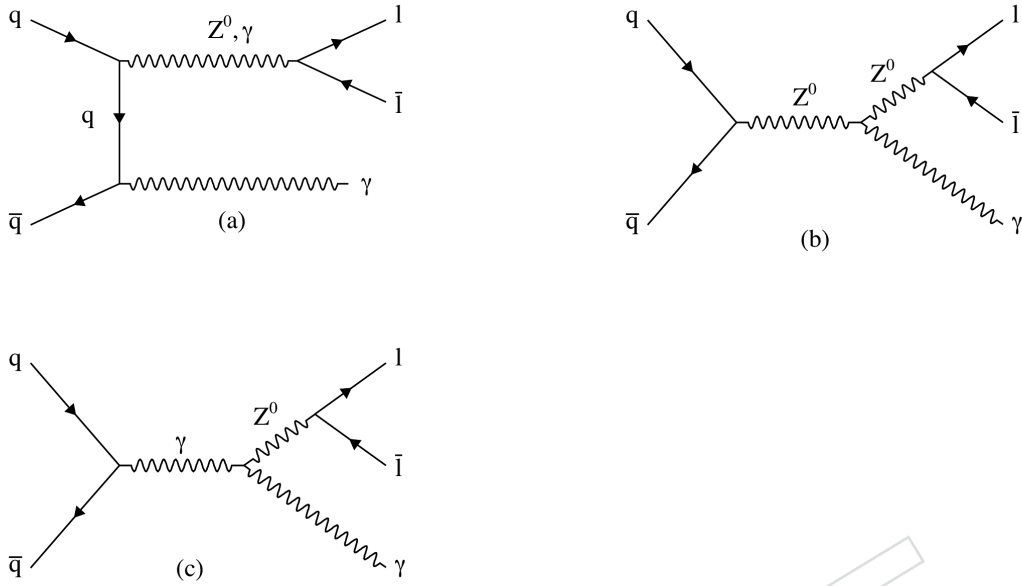


Figure 1: Feynman diagrams of the $Z\gamma$ production via initial state radiation from one of the initial state partons (a) and via the triple gauge coupling $ZZ\gamma$ (b) and $Z\gamma\gamma$ (c)

48 corresponds to an integrated luminosity of 5.0 fb^{-1} for pp collisions at $\sqrt{s} = 7 \text{ TeV}$.

49 The signal is $Z\gamma \rightarrow \nu\bar{\nu}\gamma$ where neutrino escape undetected resulting in a transverse energy
50 imbalance. Hence, the final state is photon and missing transverse energy balancing the photon.

51 The SM backgrounds for the $Z\nu\bar{\nu}\gamma$ signal are divided into two major categories: Collision and
52 non-collision photon candidates. Collision photons are from SM interactions like electroweak
53 process $W \rightarrow l\nu$ production where lepton fakes the photon, $W\gamma$ and $\gamma\gamma$ events where second
54 lepton or photon is lost. These above mentioned backgrounds are estimated from Monte Carlo.
55 The contribution from $\gamma + \pi$ multijet process, where a photon is lost and jet fakes a photon, has
56 been estimated from data.

57 The origination of Non-collision backgrounds from cosmic rays and beam effects which pro-
58 duce fake photon and missing transverse energy. Beam halo photon candidates are usually
59 produced by muons which originate upstream of the detector and travel in parallel to the beam
60 line. Those muons fake photon candidates if they interact with the electromagnetic calorimeter.
61 The shower shape and timing are the discriminators to reject this background. Similarly,
62 the contribution of photon candidates from cosmic rays is negligible after implementing these
63 discriminators to separate collision photons from cosmic ones. The contribution of beam halo
64 has been estimated from data. All these backgrounds estimation have been explained in detail
65 in later part of the paper.

66 Candidate events are selected from a data sample using a two-level trigger system, with Level-
67 1 (L1) seeding High Level Trigger (HLT). The single-photon triggers comprising this search are
68 not prescaled, and are fully efficient within the selected signal region of $|\eta^\gamma| < 1.44$ [9] and $p_T^\gamma >$
69 145 GeV . Photon candidates are restricted to be in the barrel region, where purity is highest. To
70 distinguish photon candidates from jets, we apply additional calorimetric selections. The ratio
71 of energy deposited in the HCAL to that in the ECAL within a cone $\Delta R = 0.15$ is to be less than
72 0.05. Photon candidates should have a shower distribution in the ECAL consistent with that

73 expected for a photon [9]

74 Isolation requirements on photon candidates impose upper limits on the energy deposited in
 75 the detector around the axis defined by the EM cluster position and the primary vertex [9]. In
 76 particular, the scalar sum of p_T depositions in the ECAL with in a hollow cone of $0.06 < \Delta R <$
 77 0.40 , excluding depositions within $|\eta| = 0.04$ of the cluster center, must be $< 4.2 \text{ GeV} + 0.006 \times$
 78 p_T^γ (with p_T^γ in GeV units); the sum of scalar p_T depositions in the HCAL within a hollow cone
 79 of $0.15 < \Delta R < 0.40$ must be $< 2.2 \text{ GeV} + 0.0025 \times p_T^\gamma$; and the scalar sum of tracks p_T values
 80 in a hollow cone of $0.04 < \Delta R < 0.40$, excluding depositions that are closer to the cluster center
 81 than $|\eta| = 0.015$, must be $< 2.0 \text{ GeV} + 0.001 \times p_T^\gamma$.

82 The vetoes are defined by the $|\eta|$ cutoff are needed to maintain high efficiency for photons that
 83 initiate EM showers within the tracker. The tracker isolation requirement is based on tracks
 84 that originate from the primary vertex.

85 To ensure that photon candidates are isolated from charged particle track in events with mul-
 86 tiple vertices due to high luminosity of the LHC, the tracker isolation requirement must be
 87 satisfied by all reconstructed vertices otherwise the event is being rejected.

88 The \cancel{E}_T is defined by the magnitude of the vector sum of the transverse energies of all of the
 89 reconstructed objects in the event, and is computed using a particle-flow algorithm [10]. The
 90 candidate events are required to have $\cancel{E}_T > 130 \text{ GeV}$.

91 From the moment of collisions all events are required to be deposited in the crystal that has the
 92 largest signal within $\pm 3 \text{ ns}$. This condition reduces instrumental background due to shower
 93 induced by bremsstrahlung from muons in the beam halo or in cosmic rays. Photon candidates
 94 are removed if they are likely to be electrons, as inferred from characteristic patterns of hits in
 95 the pixel detector, called "pixel seeds", that are matched to the EM cluster [11]. Furthermore,
 96 a veto was applied to events with muon candidates such as cosmic ray muons and the beam
 97 halo muon because bremsstrahlung from these muon may reconstruct an event with prompt
 98 photons balanced by missing transverse energy. Finally, events are vetoed if they contain sig-
 99 nificant hadronic activity, defined by: (i) a track with $p_T > 20 \text{ GeV}$ that is > 0.04 away from
 100 the photon candidate, or (ii) a jet that is reconstructed with $p_T > 40 \text{ GeV}$ using the anti-kT [12]
 101 particle-flow algorithm [10], within $|\eta| < 3.0$ and $\Delta R < 0.5$ of the axis of the photon.

102 After applying all of the selection criteria, 73 candidate events are found.

103 Backgrounds that are uncorelated to the collisions are estimated from data based on transverse
 104 profile of energy in the electromagnetic cluster and the the time-of-arrival of the signal in the
 105 crystal with the largest energy deposition. The Templates for anomalous signals [13], cosmic-
 106 ray muons and beam halo events are fitted to a candidate sample without timing requirement
 107 which reveals that the only significant residual contribution to the in-time sample arises from
 108 beam halo muons with an estimated 11.1 ± 5.6 events.

109 Electrons misidentified as photons arise from $W \rightarrow e\nu$ events. The matching of electron show-
 110 ers to pixel seeds has an efficiency of $\epsilon = 0.9940 \pm 0.0025$ as estimated with Monte-Carlo simu-
 111 lated events (MC) and verified with $Z \rightarrow ee$ events in data. Background is estimated by scaling
 112 a control sample of electron candidates yields an estimated contribution of 3.5 ± 1.5 events.

113 The contamination from jets misidentified as photons is estimated by using a control sample
 114 of EM-enriched QCD events to calculate the ratio of events that pass the signal photon criteria
 115 relative to those that pass looser photon criteria but fail an isolation requirement. Since the
 116 EM-enriched sample also includes production of direct single photons, this additional contri-
 117 bution to the ratio is estimated by fitting templates of energy-weighted shower widths from

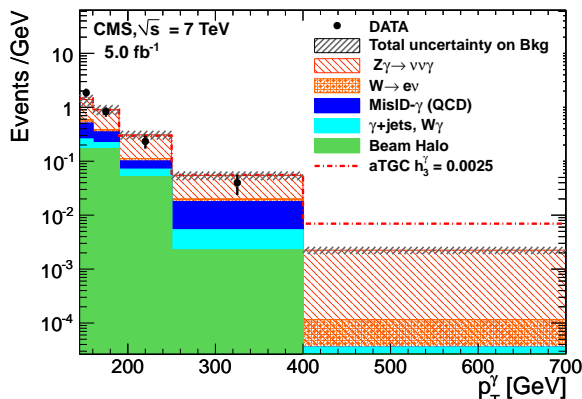


Figure 2: The photon p_T distribution for the candidate sample compared with the estimated contributions from SM background for 5 fb^{-1}

118 MC-simulated γ jets events to an independent QCD data sample, and used to subtract the γ
 119 jets contribution. This corrected ratio is applied to a subset of the EM-enriched jet events that
 120 passes loose photon identification and additional single-photon event selection criteria, pro-
 121 viding a background contribution of 11.2 ± 2.8 jet events.

122 Backgrounds from $W(l\nu)\gamma$, γ +jet, $W(l\nu)\gamma$ FSR and diphoton events are estimated from MC
 123 samples. The $W\gamma \rightarrow l\nu\gamma$ samples are generated with MADGRAPH5 [14], and the cross sec-
 124 tion is corrected to include next-to-leading order(LO) effects through a K-factor calculated with
 125 MCFM [15]. γ +jet, $W(l\nu)\gamma$ fsr and diphoton samples are obtained using the PYTHIA6.424 gen-
 126 erator [16] at leading order(LO) and CTEQ6L1 parton distribution functions(PDF). The con-
 127 tribution of MC background is about 5%, where systematic uncertainties are calculated based
 128 on acceptance times efficiency and the scale factor uncertainties which models the data-MC
 129 difference in the efficiency. The combined expected MC background event is 4.4 ± 1.1 .

130 The signal sample $Z\gamma \rightarrow \nu\bar{\nu}\gamma$ is obtained using the PYTHIA6.424 [16] and scaled up to reflect
 131 NLO contribution given in the reference [1]. The uncertainty on $Z\gamma \rightarrow \nu\bar{\nu}\gamma$ is taken as the
 132 the uncertainty on the scale factor efficiency, systematic uncertainties on the photon-vertex
 133 assignment, pile-up modeling, the accuracy of the energy calibration and photons, jet and \cancel{E}_T
 134 resolution. The expected contribution from the $Z\gamma \rightarrow \nu\bar{\nu}\gamma$ process is 45.3 ± 6.9 events. The
 135 $A \times \epsilon$ is estimated to be 0.153 ± 0.020 based on the LO simulation and includes a correction
 136 factor of $A_{NLO/LO} = 0.76 \pm 0.02$ which is applied to correct the acceptance to the NLO MC
 137 prediction based on the estimated k-factors.

138 The correction factor $\rho = 0.90 \pm 0.11$ takes into account the difference in efficiency between
 139 data and MC for the trigger, photon identification, and the veto efficiency, with systematic
 140 uncertainties. The systematic uncertainty on the measured integrated luminosity is 2.2%. The
 141 measured cross section for $Z(\nu\nu)\gamma$ is $57 \pm 11(\text{stat.}) \pm 12(\text{sys.}) \pm 1(\text{lumi.}) \text{ fb}$ which is in agree-
 142 ment with the theoretical prediction at NLO of $59 \pm 3 \text{ fb}$.

143 Given the good agreement of both the measured cross sections and the photon p_T distributions
 144 with the corresponding SM predictions (Figure 2), we set limits on anomalous TGCs. Simulated
 145 samples of $Z\gamma$ signal for a grid of aTGCs values are produced using SHERPA Monte-Carlo. A
 146 grid of h_3 and h_4 values is used for the $ZZ\gamma$ and $Z\gamma\gamma$ couplings. Assuming Poisson statistics
 147 and log-normal distributions for the generated samples and background systematic uncertain-
 148 ties, we calculate the likelihood of the observed photon p_T spectrum in data given the sum
 149 of the background and aTGCs p_T^γ predictions for each point in the grid of aTGCs values. To

150 extract limits we parametrize the expected yields as a quadratic function of the anomalous couplings.
 151 We then form the probability of observing the number of events seen in data in a given
 152 bin of the photon transverse momentum using a Poisson distribution with the mean given by
 153 the expected signal plus a data driven background estimate and allowing for variations within
 154 the systematic uncertainties. The confidence intervals are found using MINUIT, profiling the
 155 likelihood with respect to all systematic variations [17]. The resultant one-dimensional 95%
 156 confidence level (CL) limits are given in figure 3 and figure 4.

157 To set the limits on CLs criteria, the tool developed by Higgs PAG [18] has been implemented.
 158 Furthermore, one-dimensional 95% CL limits on a given anomalous coupling, we set the other
 159 aTGCs to their respective SM predictions. The results are summarized in Table 1.

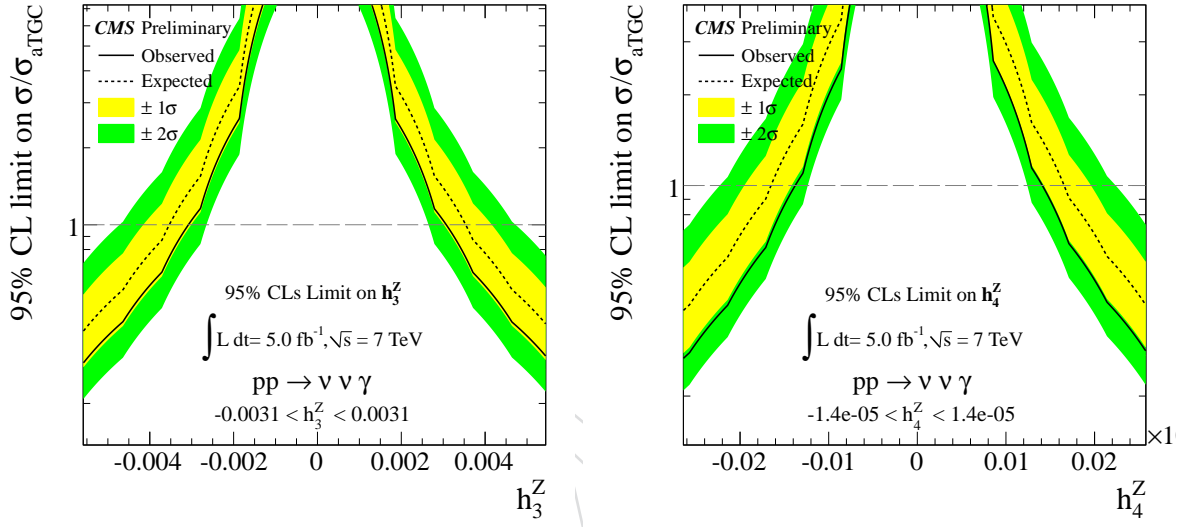


Figure 3: 1 D limit using Higgs tool for $ZZ\gamma$ (a) and (b) couplings without pile up correction in isolation

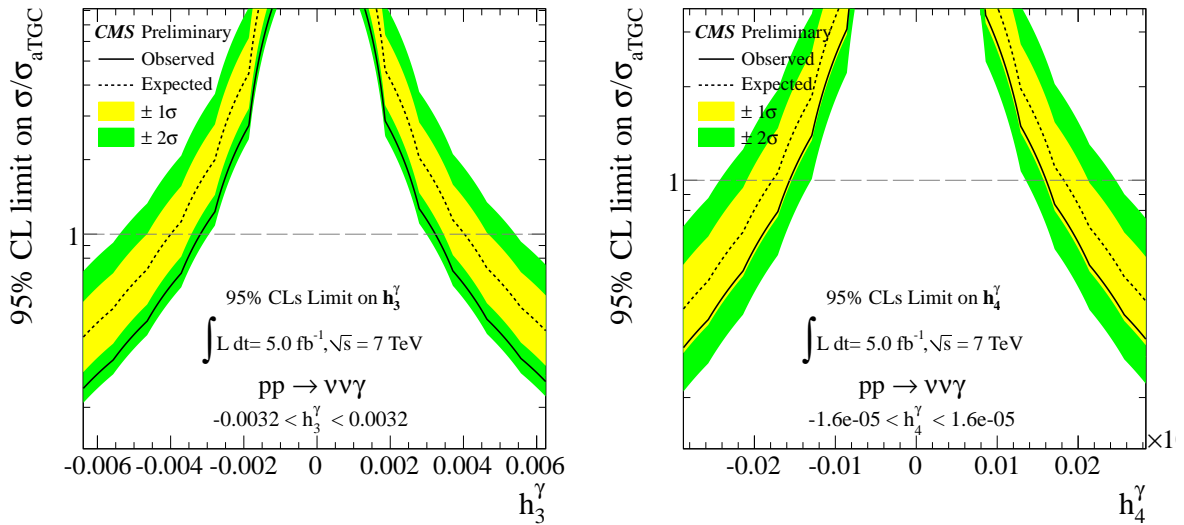


Figure 4: 1 D limit using Higgs tool for $Z\gamma\gamma$ couplings without pile up correction in isolation

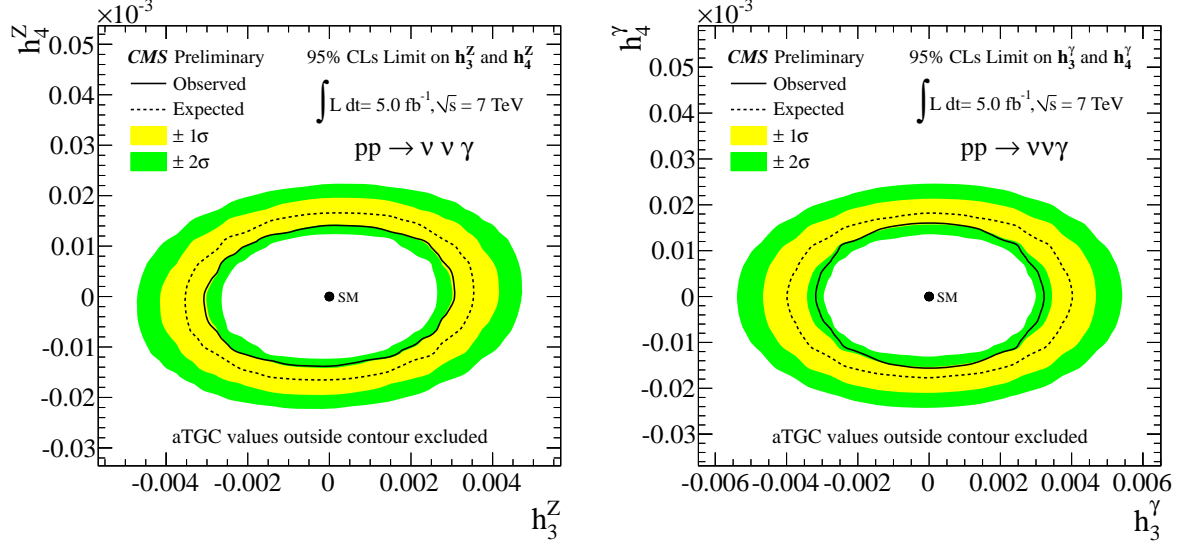


Figure 5: 2 D contour plot Higgs tool for $ZZ\gamma$ couplings (a) and $Z\gamma\gamma$ (b) without pile up correction in isolation

Coupling	h_3 Lower limit 10^{-3}	h_3 Upper Limit 10^{-3}	h_4 Lower limit 10^{-5}	h_4 Upper Limit 10^{-5}
Neutrino Channel				
$Z\gamma\gamma$	-3.2	3.2	-1.6	1.6
$ZZ\gamma$	-3.1	3.1	-1.4	1.4

Table 1: One-dimensional limits on $Z\gamma$ anomalous trilinear gauge couplings using Higg's Tool for neutrino channels in CMS

160 In conclusion, we find that the p_T^γ distribution of photons produced in Z boson in neutrino
 161 decay channel in a data sample corresponding to an integrated luminosity of 5 fb^{-1} . We place
 162 95% CLs limits of $|h_3| < 3.2 \times 10^{-3}$ ($h_4 = 0$) and $|h_4| < 1.6 \times 10^{-5}$ on CP-conserving parameter
 163 without no form factor scale. While limits for $Z\gamma\gamma$ couplings are $|h_3| < 3.1 \times 10^{-3}$ ($h_4 = 0$) and
 164 $|h_4| < 1.4 \times 10^{-5}$. These are significantly tighter constraints on the BSM contributions than
 165 those provided by leptonic channels [19].

References

- 166
- 167 [1] U. Baur And- E. Berger, “Probing the weak-boson sector in $Z\gamma$ production at hadron
168 colliders”, *Phys. Rev.* **D47** (1993) 4889. doi:10.1103/PhysRevD.47.4889.
- 169 [2] V. Abazov, et al, “ $Z\gamma$ production and limits on anomalous $ZZ\gamma$ and $Z\gamma\gamma$ couplings in pp
170 collisions at $\sqrt{s} = 1.96$ TeV”, *Phys. Rev.* **D 85** (2012) 052001.
171 doi:10.1103/PhysRevD.85.052001.
- 172 [3] T. Aaltonen et al(CDF Collaboration), “Limits on Anomalous Trilinear Gauge Couplings
173 in $Z\gamma$ Events from the $p\bar{p}$ collisions at $\sqrt{s} = 1.96$ TeV”, *Phys. Rev. Lett.* **107** (2011) 051802.
174 doi:10.1103/PhysRevLett.107.051802.
- 175 [4] DELPHI Collaboration, “Study of Triple-Gauge-Boson Couplings ZZZ , $ZZ\gamma$, $Z\gamma\gamma$ at
176 LEP”, *Eur. Phys. J. C* **51** (2007) 525–542. doi:10.1140/epjc/s10052-007-0345-0.
- 177 [5] P.Achard et al. (L3 Collaboration), “Study of $e + e^- \rightarrow Z\gamma$ process at LEP and limits on
178 triple neutral-gauge-boson couplings”, *Phys. Lett.* **B 597** (2004) 119.
- 179 [6] CMS Collaboration, “Measurement of $W\gamma$ and $Z\gamma$ production in pp collisions at $\sqrt{s} = 7$
180 TeV”, *Physics Letter B* **701** (2011) 535–555.
- 181 [7] ATLAS Collaboration, “Measurement of $W\gamma$ and $Z\gamma$ production cross sections in pp
182 collisions at $\sqrt{s} = 7$ TeV and limits on anomalous triple gauge couplings with the ATLAS
183 detector”, *Submitted to Physics Letter B.* doi:arXiv:1205.2531v1.
- 184 [8] CMS Collaboration, “CMS technical design report, volume II: Physics Performance”,
185 *J. Phys.G: Nucl. Part.Phys.* **34** (2007) 995. doi:10.1088/0954-3899/34/6/S01.
- 186 [9] CMS Collaboration, “Isolated Photon Reconstruction and Identification at $\sqrt{s} = 7$ TeV”,
187 *CMS Physics Analysis Summary CMS-PAS-EGM-10-006* (2011).
- 188 [10] CMS Collaboration, “Commissioning of the Particle-Flow Reconstruction in Minimum
189 -Bias and Jet Events from pp Collisions at $\sqrt{s} = 7$ TeV”, *CMS Physics Analysis Summary*
190 *CMS-PAS-PFT-10-002* (2010).
- 191 [11] CMS Collaboration, “Electron Reconstruction and Identification at $\sqrt{s} = 7$ TeV”, *Physics*
192 *Analysis Summary CMS-PAS-EGM-10-004* (2010).
- 193 [12] M. Cacciari, G.P. Salam, and G. Soyez, “The anti- k_T jet clustering algorithm”, *JHEP* **04**
194 (2008) 063. doi:arXiv:0802.1189. doi:10.1088/1126-6708/2008/04/063.
- 195 [13] A. Askew et al, “Search for New Phenomena with Mono-Photon and Missing Transverse
196 Energy Final State in pp Collisions at $\sqrt{s} = 7$ TeV”, *CMS Analysis Note 2011/108* (2011).
- 197 [14] J. Alwall, M. Herquet, F. Maltoni et al, “MadGraph 5: Going Beyond”, *JHEP* **6** (2011) 128.
198 doi:10.1007/JHEP06(2011)128.
- 199 [15] J. Campbell, R. Ellis, and C. Williams, “MCFM v6.1: A Monte Carlo for FeMtobarn
200 processes at Hadron Colliders”, *A Monte Carlo for FeMtobarn processes at Hadron Colliders*
201 (2011).
- 202 [16] J. Sjostrand, S. Mrenna, and P.Z. Skands, “PYTHIA6.4 Physics and Manual”, *JHEP* **5**
203 (2006) 26. doi:arXiv:hep-ph/0603175.
204 doi:10.1088/1126-6708/2006/05/026.

- 205 [17] Particle Group Collaboration, “Review of particle physics Section 33.3.2.3”, *J. Phys.* **G37**
206 (2010) 075021. doi:doi:10.1088/0954-3899/37/7A/075021.
- 207 [18] <https://twiki.cern.ch/twiki/bin/viewauth/CMS/SWGuideHiggsAnalysisCombinedLimit>.
- 208 [19] CMS Collaboration, “Study of $W\gamma$ and $Z\gamma$ production at CMS with $\sqrt{s} = 7\text{TeV}$ ”, *CMS*
209 *Analysis Note AN-2011-251* (2011).

DRAFT